Tetrahedron 67 (2011) 3677–3684

Contents lists available at ScienceDirect

Tetrahedron

journal homepage: www.elsevier.com/locate/tet

Structural study of oxalamide compounds: ^{1}H, ^{13}C, and DFT calculations

Abdelkarim El Moncef, Elena Zaballos *, Ramón J. Zaragozá *

Departamento de Química Orgánica, Universidad de Valencia, Dr. Moliner 50, 46100 Burjassot, Valencia, Spain

ARTICLE INFO

Article history:
Received 22 February 2011
Received in revised form 22 March 2011
Accepted 22 March 2011
Available online 30 March 2011

Keywords:
Oxalamides
Oxamides
DFT calculations
^{13}C and ^{1}H NMR spectra
GIAO method

ABSTRACT

The conformational properties of some *N*-alkyl, *N*,*N*′-dialky, and tetraalkyloxalamides have been investigated, in vacuo and in solvent using DFT methods at the B3LYP/6-31G** computational level. Special emphasis has been given on oxalamides with substituents of the type $-CH_2CH_2OH$. In oxalamides with the N–H group (*N*-alkyl and *N*,*N*′-dialky), the most stable conformations are those in which the oxalamide moiety adopts a planar *s-trans* arrangement and the amide bonds are *trans*. A different situation appears in the case of tetraalkyloxalamides, in which the oxalamide moiety always adopts a skewed arrangement and there are conformations with similar energy. A careful study of ^{13}C and ^{1}H NMR spectra together with theoretical calculations (GIAO method) allowed the assignment of the signals of these conformers. The presence of the $-CH_2CH_2OH$ chain produces numerous rotamers. The most stable rotamers, in vacuo, are those with strong intramolecular hydrogen bonds, however in solvent, hydrogen bonds are not crucial to establish the most stable specie and depend on the solvent used.

1. Introduction

The new retro-bispeptides having the oxalamide moiety located at the center has become of great interest. The retro-bispeptides have been used in protein engineering to generate non coded α-amino acids[1] as well as to prepare bioactive peptides with enhanced stability toward enzymatic degradation.[2] Moreover, oxalamide linkages are also of great importance in the material science field, since they are included in the aliphatic polyamides,[3,4] i.e., nylons.

On the other hand, the bis(amino acid)- and bis(amino alcohol)-oxalamide gelators represent the class of versatile gelators whose gelation ability is a consequence of strong and directional intermolecular hydrogen bonding provided by oxalamide units.[5]

Understanding of the molecular and electronic structure of the oxalamide group is essential to explain the conformational properties and dynamics of the molecules containing the oxalamide moiety.

Oxalamide moiety may exist in two extreme dispositions, *s-cis* or *s-trans*, respect to the dicarbonylic function. It is well known the greater stability of the *s-trans* arrangement, however the CO–CO torsion angle (ω_2 in Scheme 1) in many cases takes a value of 180° (pure *s-trans*), but in others it may vary between 90° and 180°.[6–9] In addition, the rotation around the CO–N amide bond (ω_1 or ω_3 in Scheme 1) gives rise to several conformers. The result is a complex mixture of conformers, some of which can be observed in the ^{1}H and ^{13}C NMR spectra. For example, *N*,*N*′-dialkyloxalamides show a simple spectrum,[10] but the NMR spectra of tetraalkyloxalamides are more complex due to the presence of several conformers of similar stability.[10,11]

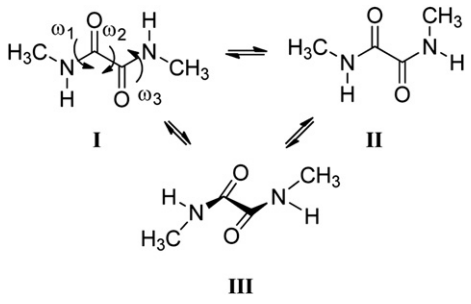

Scheme 1. Low-energy conformations of *N*,*N*′-dimethyloxalamide.

To our knowledge, only few systematic conformational studies have been conducted in oxalamides. The conformational properties of the simple *N*,*N*′-dimethyloxalamide have been studied in different environments using theoretical methods.[12,13] There are three minimum energy conformations, **I**–**III** in Scheme 1.

The lowest energy minimum corresponds to the conformer **I**, in which the two dihedral angles O=C–N–H (ω_1 and ω_3) are 180° and the O=C–C=O torsion angle (ω_2) adopt a planar *s-trans* conformation. The conformer **II** (ω_1 or ω_3=0°), is 6.2 kcal/mol higher in energy than the conformer **I**. Finally, the less stable minimum

* Corresponding authors. Tel.: +34 963543040; fax: +34 963544328 (R.J.Z.); tel.: +34 963543047; fax: +34 963544328 (E.Z.); e-mail addresses: elena.zaballos@uv.es (E. Zaballos), ramon.j.zaragoza@uv.es (R.J. Zaragozá).

0040-4020/$ – see front matter © 2011 Elsevier Ltd. All rights reserved.
doi:10.1016/j.tet.2011.03.075

(12.7 kcal/mol relative to **I**) corresponds to the conformer **III** (ω_1 and ω_3=0°), in which the central dihedral angle ω_2 adopts a *skew* conformation with a value of 145°. Due to the large difference in stability of the conformer **I** toward **II** and **III**, this is the only conformation observed in the ^{1}H and ^{13}C NMR spectrums.

In the present paper, a systematic and detailed conformational study as well as an NMR study has been made with different oxalamides and particular emphasis has been made on oxalamides with substituents of the type $-CH_2CH_2OH$. In these cases the conformational study is very complex due to the presence of several rotamers of the $-CH_2CH_2OH$ chain and the possibility of hydrogen bonds (HB) between the hydroxyl and other functional groups present in the structure.

The theoretical study has been carried out in vacuum and in several solvents in order to study the conformational and HB changes in different media. A careful study of ^{13}C and ^{1}H NMR spectra together with theoretical calculations (GIAO method) has been made to allocate spectrum signals corresponding to different conformers.

For the study of the oxalamides, five models (Scheme 2) were chosen, grouped in two groups. The first group (compounds **1** and **2**) corresponds to oxalamides with at least two N–H moieties and the second group (compounds **3**–**5**) corresponds to tetra alkyl oxalamides. The compounds **1**, **3**, and **4** are simple models used to simplify the subsequent study of more complex compounds **2** and **5**.

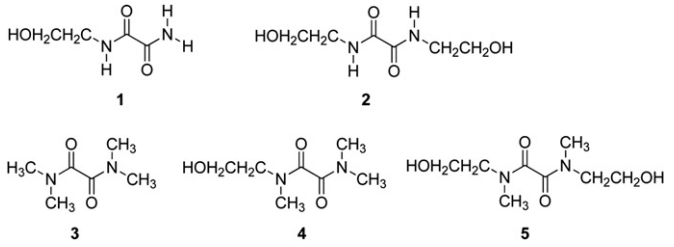

Scheme 2. Models under study.

2. Computational methods

All calculations were carried out with the Gaussian 03 suite of programs.[14] Density functional theory[15] calculations (DFT) have been carried out using the B3LYP[16] exchange-correlation functionals, together with the standard 6-31G** basis set.[17] The inclusion of solvent effects has been considered by using a relatively simple self-consistent reaction field (SCRF) method[18] based on the polarizable continuum model (PCM) of Tomasi's group.[19] Geometries have been fully optimized with PCM. The solvent we have used was Cl_3CH (common solvent in NMR spectroscopy) and also dimethylsulfoxide (DMSO) or CH_3OH. NMR calculations of absolute shielding using gauge including atomic orbital method (GIAO) were carried out using 6-311++G** as basis set.

3. Results and discussion

Before starting the study of oxalamides, we consider interesting to clarify the terminology used in this paper. There were some confusions and inconsistencies about the naming of conformers in amide groups in the existing literatures. We will follow the definition such that the *cis* or *trans* conformer is defined by the dihedral angle made by CO–CO and N–R bonds around the central CO–N bond (R=highest priority group). Additionally we use the term 'conformer' when we refer to conformers resulting from rotation of the CO–N amide bonds and 'rotamers' when we refer to conformers resulting from rotation of the side chains or CO–CO bond.

3.1. Models 1 and 2

*3.1.1. Model **1**: N-(2-hydroxyethyl)oxalamide.* The presence of two different substituents on the N1 atom means that there are two conformations as a result of rotation of the amide ω_1 bond, the **t** (*trans*) and the **c** (*cis*) in Scheme 3. The rotation around N1–C7, C7–C8, C8–O9 and the possibility of HB between the hydroxyl and other functional groups present in the structure, increase the number of rotamers.

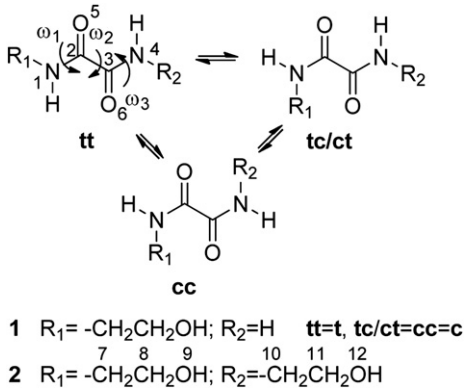

Scheme 3. Different conformations of *N*-(2-hydroxyethyl)oxalamide (**1**) and *N*,*N*′-bis (2-hydroxyethyl)oxalamide (**2**).

We have made an extensive conformational study, in vacuo and in Cl_3CH, for *N*-(2-hydroxyethyl)oxalamide (**1**). Fig. 1 shows the geometries (optimized in Cl_3CH) and Table 1 the energies of the more relevant conformers. The inclusion of the solvent does not produce significant geometric changes. **1ta**–**1tf** rotamers have a *trans* disposition around the amide ω_1 bond (Notation used: **1**=Model; **t**=*trans*; **a**,**b**…=rotamer). The two five-membered rings formed by hydrogen bonding, N1–H···O6 and N4–H···O5, allows the flat arrangement of the oxalamide group (dihedral angle O=C–C=O about 180°). **1ca** (Notation used: **c**=*cis*) is the more relevant rotamer with *cis* geometry and due to the absence of the N1–H···O6 HB and the appearance of the O9–H···O6 HB (bond length=1.90 Å), adopt a *skew* conformation (dihedral angle O=C–C]O is 163°).

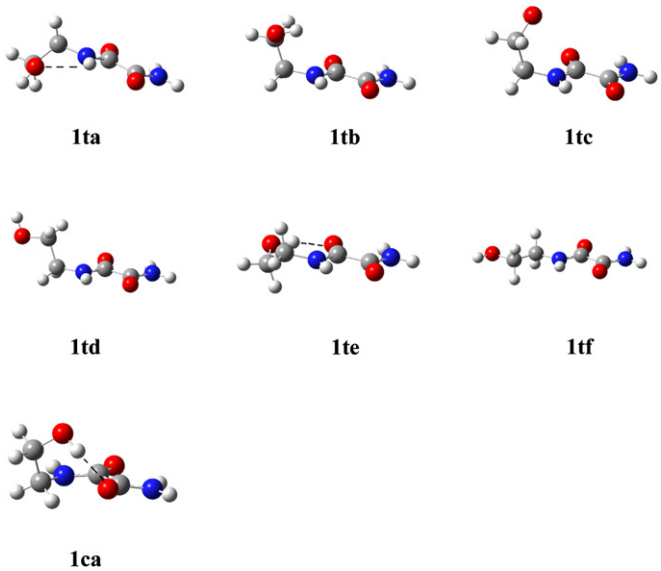

Fig. 1. Geometries of the more relevant stationary points involved in the conformational study of *N*-(2-hydroxyethyl)oxalamide (**1**) in Cl_3CH. Strong HB are shown.

Table 1
B3LYP/6-31G** Relative free energies (ΔG, in kcal/mol, 298.15 K, 1 atm) in vacuo (ΔG_{vacuo}), Cl_3CH (ΔG_{Cl_3CH}) and free energies of solvation (ΔG_{sol}) of the stationary points involved in the conformational study of *N*-(2-hydroxyethyl)oxalamide (**1**)

	ΔG_{vacuo}	ΔG_{Cl_3CH}	ΔG_{sol}[a]
1ta	0.8	0.0	−12.8
1tb	1.0	0.7	−12.2
1tc	1.0	1.1	−11.8
1td	2.2	1.4	−12.7
1te	0.0	1.7	−10.2
1tf	4.5	3.7	−12.7
1ca	5.7	6.6	−11.0

[a] Obtained by difference between the free energies in Cl_3CH and in vacuo.

As you can see from the Table 1, *trans* rotamers (**1ta**–**1tf**) are more stable than *cis* rotamer **1ca**. **1ta** presents an HB N1–H···O9 with a bond length of 2.57 Å. In **1tb**, **1tc**, and **1td**, the $-CH_2OH$ is situated perpendicular to the plane formed by the oxalamide group, and correspond to the three staggered conformations resulting from rotation of the CH_2-CH_2OH bond. **1tb** and **1tc** have a weak HB between O9–H···N1 (bond length=2.84 Å) and O9–H···O5 (bond length=2.98 Å), respectively. The rotamer **1te** present a strong HB O9–H···O5 with a bond length of 1.84 Å. Finally, **1tf** corresponds to the rotamer in which the bulky groups are located in an *anti* arrangement and is the most unstable of all *trans* rotamers.

Looking at Table 1, we can see that the energy of **1ta** to **1te** differs depending on the actual calculations are in vacuo or in Cl_3CH. In vacuo, most stable rotamers are those with strong HB. The energy of rotamers follows the order **1te**<**1ta**<**1tb**<**1tc**<**1td**, consistent with the greater strength of intramolecular HB. Due to increasing polarity by the presence of the hydroxyl group, the inclusion of the solvent produces a strong stabilization of all rotamers (between 10.2 and 12.8 kcal/mol). This stabilization is lower in rotamers with strong intramolecular HB (see **1te**). Therefore, in chloroform, intramolecular HB are not crucial to establish the most stable rotamer.[20] In fact, the most stable rotamer corresponds to **1ta**, closely followed by **1tb** (0.7 kcal/mol). These energy values indicate that, in chloroform, **1** will exist primarily as *trans* conformer with a fast conformational exchange between all *trans* rotamers, predominant **1ta** and **1tb**. The ^1H and ^{13}C NMR spectra will be simple and without duplication of signals.

*3.1.2. Model **2**: N,N′-bis(2-hydroxyethyl)oxalamide.* In this compound (Scheme 3) there are three main conformations, resulting from rotation of the ω_1 and ω_3 bonds, corresponding to *trans*–*trans* (**tt**), *trans*–*cis* or *cis*–*trans* (**tc**/**ct**), and *cis*–*cis* (**cc**) conformers. In addition, each of these conformations will have a large number of rotamers resulting from rotation of the $-CH_2CH_2OH$ chain. To simplify, we have to assume that the more stable conformer will be the **tt**, as happens with the *N,N′*-dimethyloxalamide (see Scheme 1). This assumption is also supported by the difference in stability observed in the *trans* rotamers **1ta**–**1tf** in front of the *cis* rotamer **1ca** (see model **1**).

We have made an extensive conformational study for the **tt** conformer, but to simplify we only show the symmetric rotamers **2tta**–**2ttc**. These rotamers are similar to **1ta**, **1te**, and **1tb**, respectively, in model **1**. Dues to the insolubility of **2** in chloroform, their experimental spectra have been recorded in deuterated dimethylsulfoxide (DMSO-d_6). Therefore, the conformational study has been made in vacuo, Cl_3CH and in DMSO. Fig. 2 shows the geometries (optimized in Cl_3CH) and Table 2 the energies of the more relevant rotamers (**2tta**–**2ttc**).

The three rotamers **2tta**–**2ttc** adopt a flat arrangement of the oxalamide group (dihedral angle O=C–C=O about 180°) with two five-membered rings formed by hydrogen bonding, N1–H···O6 and N4–H···O5. In addition, **2ttb** has two identical strong HB

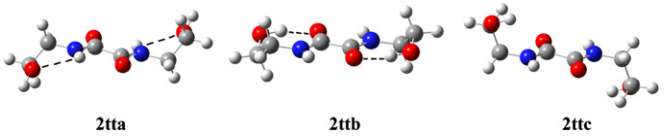

Fig. 2. Geometries of the more relevant stationary points involved in the conformational study of *N,N′*-bis(2-hydroxyethyl)oxalamide (**2**) in Cl_3CH. Strong HB are shown.

Table 2
B3LYP/6-31G** Relative free energies (ΔG, in kcal/mol, 298.15 K, 1 atm) in vacuo (ΔG_{vacuo}), Cl_3CH (ΔG_{Cl_3CH}), DMSO (ΔG_{DMSO}) and free energies of solvation (ΔG_{sol}) of the stationary points involved in the conformational study of *N,N′*-bis(2-hydroxyethyl)oxalamide (**2**)

	ΔG_{vacuo}	ΔG_{Cl_3CH}	ΔG_{sol}[a]	ΔG_{DMSO}	ΔG_{sol}[b]
2tta	1.7	0.0	−12.5	0.3	−17.2
2ttb	0.0	0.8	−9.9	1.4	−14.4
2ttc	2.0	0.1	−12.8	0.0	−17.8

[a] Obtained by difference between the free energies in Cl_3CH and in vacuo.
[b] Obtained by difference between the free energies in DMSO and in vacuo.

O9–H···O5 and O12–H···O6 (seven-membered rings) with a bond length of 1.85 Å, being the most stable rotamer in vacuo. **2tta** has two additional five-membered rings formed by N–H···O HB (bond length=2.55 Å). This rotamer has two three-center hydrogen bonding interaction (THB), O9···H1···O6, and O12···H4···O5.[21]

Again, the inclusion of the solvent does not produce significant geometric changes; however it produces a strong stabilization of all species (between 9.9 and 12.8 kcal/mol in Cl_3CH and between 14.4 and 17.8 kcal/mol in DMSO), being this stabilization lesser in **2ttb** with strong intramolecular HB. The result is that in Cl_3CH the most stable rotamer is the **2tta** while in DMSO is **2ttc**.

3.1.2.1. NMR study of N,N′-bis(2-hydroxyethyl)oxalamide. As seen above, oxalamide **2**[22] in solution (Cl_3CH or DMSO) will be mainly as a mixture of several rotamers (**2tta**–**2ttc** among others) of the **tt** conformer. The rapid exchange between the rotamers (**2tta**–**2ttc**), at room temperature, produces a single spectrum.[23] The ^1H and ^{13}C NMR spectra, as consequence of the symmetry of the molecule, have half of the signals (see Supplementary data). The ^{13}C NMR spectra, in DMSO-d_6, show only three signals. The amidic carbon chemical shifts at 160.2 ppm appear at higher field that the chemical shifts of a monoamide (about 170 ppm). This indicates that the nitrogen lone pair is delocalized over the π-system of the adjacent carbonyl bond.[24] The signals of C8/C11 atoms are observed at 59.4 ppm and those of C7/C10 at 41.8 ppm.

In the ^1H NMR, in DMSO-d_6, four signals appear. The amide N1–H/N4–H protons display a triplet signal at 8.56 ppm (*J* 5.8 Hz) by coupling with methylene protons (C7–H_2/C10–H_2). The O9–H/O12–H protons appear at 4.76 ppm as a broad singlet. The triplet (*J* 6.2 Hz) at 3.45 ppm corresponds to the C8–H_2/C11–H_2 methylene protons. And finally, the methylene protons C7–H_2/C10–H_2 appear at 3.22 ppm as a quadruplet (*J* about 6 Hz). This last signal is, in reality, a double triplet overlapped due to the coupling with the near methylene protons (triplet, *J* 6.2 Hz) and the amidic protons (triplet, *J* 5.8 Hz), with almost the same constants coupling.

DMSO, can exert a dominant influence on the N–H hydrogen bonding behavior, acting as a proton quencher. The conformation in the $-CH_2CH_2OH$ chains exert a strong effect on the chemical shift of the amide N–H protons. The N–H signal at 8.56 ppm points to a highly flexible side chain without the formation of strong HB between the OH and NH,[6] in accordance with the theoretical results. In this case, the formation of the THB interaction (see **2tta**) in the stabilization of **2** in DMSO, seems to be not relevant.

Further evidence of the role played by THB interaction was given by the temperature dependence coefficients ($-\Delta\delta/\Delta T$ in ppb K^{-1}) of

the N–H chemical shift resonances in DMSO.[6–8,21,25] Small values of $-\Delta\delta/\Delta T$ (below 3 ppb), for the N–H hydrogen, is typical of systems with intramolecular HB, and support the formation of THB in oxalamides. By contrast, high values ($-\Delta\delta/\Delta T$ above 4 ppb) correspond to solvated N–H groups.[7,8]

The spectra of the oxalamide **2** were recorded, in DMSO-d_6, at 298, 325, 350, 375, 400, and 425 K, and the results are shown in Fig. 3. The experimental value of $-\Delta\delta/\Delta T$=5.2 (±0.3) ppb K^{-1} discard the formation of a strong intramolecular hydrogen bonding between the N–H and O–H groups, due to solvation of the N–H group with DMSO. These results are again in agreement with theoretical studies.

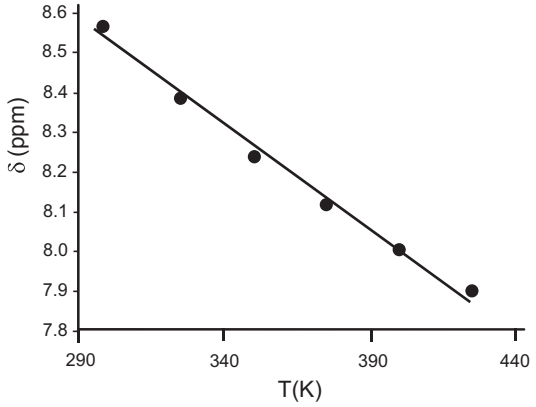

Fig. 3. δ as a function of T(K) for the amide protons of *N*,*N*′-bis(2-hydroxyethyl)oxalamide (**2**) in DMSO.

It should be noted that with increasing temperature, the signal of the N–H group becomes a broad singlet. It also shows the variation of the methylene protons C7–H_2/C10–H_2 signal, which at 425 K turns into a triplet. As the temperature rises, the rapid intermolecular exchange between protons of the N–H group prevents the coupling with the methylene group.

3.2. Models 3–5

*3.2.1. Model **3**: tetramethyloxalamide.* Due to the presence of four identical substituents on the nitrogen atom, the four conformations (**tt**, **tc**, **ct**, and **cc** in Scheme 4) resulting from rotation of the amide bond, are equal. With this simple model we have carried out, in vacuo and in Cl_3CH, a detailed conformational and rotational theoretical study (see Scheme 5). Fig. 4 shows the geometries (optimized in Cl_3CH) of conformations (**3a**=**3a**′ and **3b**) and transition states (**TS1**, **TS2***syn*, and **TS2***anti*) involved in the rotation around amide bond (ω_1 or ω_3) and CO–CO bond (ω_2). The energies of the relevant species are in Table 3.

The tetramethyloxalamide can adopt two staggered rotamers resulting from rotation of the CO–CO bond (**3a** and **3b**). Both rotamers have an axis of chirality, are two enantiomeric conformations and therefore isoenergetic. The dihedral angle O=C–C=O is 110° and −110° for **3a** and **3b**, respectively. The two nitrogen atoms retain almost perfect planar geometry in both rotamers.

The free energy of activation in vacuo for **3a**–**3b** interconversion is equal to 4.8 kcal/mol and corresponds to the **TS1**. In the transition state **TS1**, the oxalamide group adopts a planar arrangement, that is, the dihedral angle O=C–C=O is 180° and nitrogen atoms retain planar geometry. The low energy barrier associated with this **TS** allows a rapid exchange between the two rotamers at room temperature.

Rotation around the amide bond (ω_1 or ω_3) can lead to two possible transition states, **TS2***syn* and **TS2***anti*, with *syn* or *anti* orientation between the carbonyl oxygen and the nitrogen lone

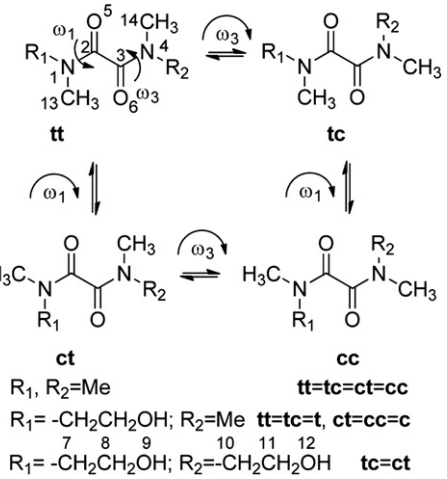

Scheme 4. Different conformations of tetramethyloxalamide (**3**), *N*-(2-hydroxyethyl)-*N*,*N*′,*N*′-trimethyloxalamide (**4**) and *N*,*N*′-bis(2-hydroxyethyl)-*N*-*N*′-dimethyloxalamide (**5**).

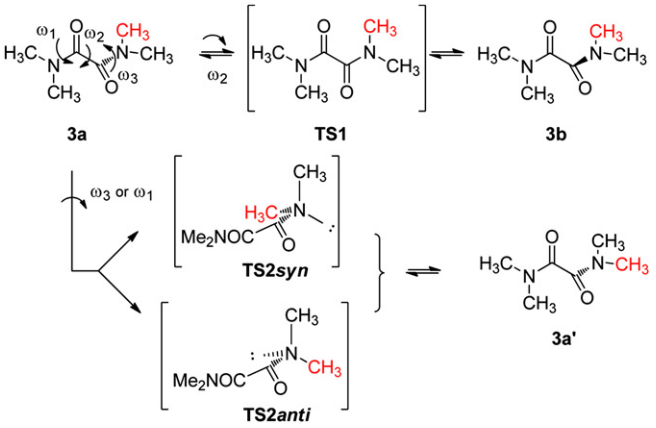

Scheme 5. Different conformations and **TS** resulting from rotation of the amide and CO–CO bonds in tetramethyloxalamide (**3**).

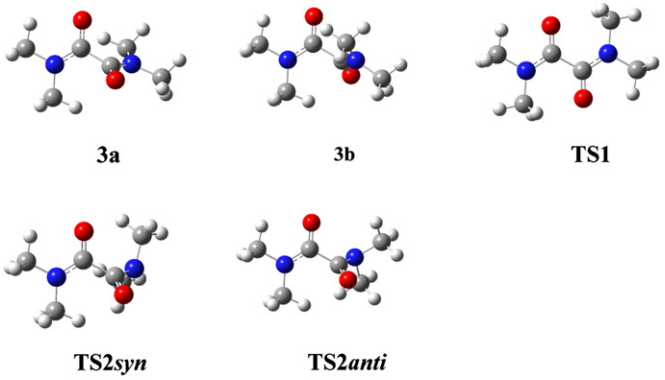

Fig. 4. Geometries of the stationary points involved in the conformational study of tetramethyloxalamide (**3**) in Cl_3CH.

pairs. In both transition states, nitrogen adopts a sp^3 hybridization, and therefore, a pyramidal conformation. The free energy of activation associated with these two transition states in vacuo are 21.7 kcal/mol for **TS2***syn* and 20.9 kcal/mol for **TS2***anti*. Thus, **TS2***anti* is about 0.8 kcal/mol more stable than **TS2***syn*. This difference may be due to electronic repulsion between the lone pair of electrons of nitrogen and carbonyl oxygen electron pairs in the **TS2***syn*. These energy values are close to those found for *N*,*N*′-

Table 3
B3LYP/6-31G** Relative free energies (ΔG, in kcal/mol, 298.15 K, 1 atm) in vacuo (ΔG_{vacuo}), Cl_3CH (ΔG_{Cl_3CH}) and free energies of solvation (ΔG_{sol}) of the stationary points involved in the conformational study of tetramethyloxalamide (**3**)

	ΔG_{vacuo}	ΔG_{Cl_3CH}	ΔG_{sol}[a]
3a	0.0	0.0	−5.8
3b	0.0	0.0	−5.8
TS1	4.8	7.1	−3.6
TS2*syn*	21.7	23.3	−4.2
TS2*anti*	20.9	22.3	−4.5

[a] Obtained by difference between the free energies in Cl_3CH and in vacuo.

dimethyloxalamide[13] and for a typical amide bond.[26] This high rotational barrier slows down the exchange between the two conformers (**3a** and **3a′**). This means that in the case of two different alkyl substituents on nitrogen, both conformers can be observed in NMR spectra.

The inclusion of the solvent (Cl_3CH) stabilizes all species between 3.6 and 5.8 kcal/mol. This stabilization is greater in **3a** and **3b** with respect to **TS**s and the overall result is an increase in rotational energy barriers.

*3.2.2. Model **4**: N-(2-hydroxyethyl)-N,N′,N′-trimethyloxalamide.* As in the model **1**, the presence of two different substituents on the N1 atom means that there are two conformations as a result of rotation of the amide ω_1 bond, the *trans* (**t**) and the *cis* (**c**) in Scheme 4. There will also be a large number of rotamers as a result of the rotation around N1–C7, C7–C8, C8–O9 bonds and the possibility of HB between the hydroxyl and other functional groups present in the structure. In addition, due to predictable loss of planarity in the oxalamide group, the compound can adopt several staggered rotamers resulting from rotation of the CO–CO bond.

The conformational study has been made in vacuo and in Cl_3CH, for *N*-(2-hydroxyethyl)-*N*,*N*′,*N*′-trimethyloxalamide (**4**). Fig. 5 shows the geometries (optimized in Cl_3CH) and Table 4 the energies of the more relevant conformers.

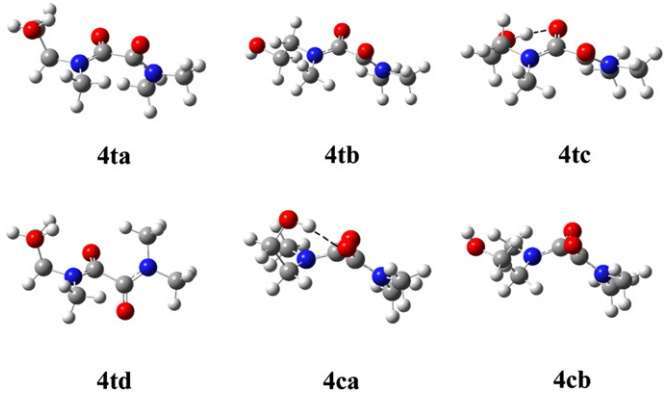

Fig. 5. Geometries of the more relevant stationary points involved in the conformational study of *N*-(2-hydroxyethyl)-*N*,*N*′,*N*′-trimethyloxalamide (**4**) in Cl_3CH. Strong HB are shown.

4ta–**4td** corresponds to different rotamers all with a *trans* disposition around the amide ω_1 bond. **4ca** and **4cb** are the more relevant rotamers with *cis* geometry. Due to the absence of the N–H···O=C HB, all conformers adopt a *skew* disposition as a result of rotation of the ω_2 bond. **4ta**–**4tc** and **4ca**–**4cb** have a similar skewed arrangement, with a dihedral angle O=C–C=O between 109° and 115°. Each of these conformers has a corresponding staggered rotamer with a negative dihedral angle O=C–C=O and energy greater or similar to those shown. As an example of rotamer with a negative dihedral angle, the Fig. 5 shows **4td** that

Table 4
B3LYP/6-31G** Relative free energies (ΔG, in kcal/mol, 298.15 K, 1 atm) in vacuo (ΔG_{vacuo}), Cl_3CH (ΔG_{Cl_3CH}) and free energies of solvation (ΔG_{sol}) of the stationary points involved in the conformational study of *N*-(2-hydroxyethyl)-*N*,*N*′,*N*′-trimethyloxalamide (**4**)

	ΔG_{vacuo}	ΔG_{Cl_3CH}	ΔG_{sol}[a]
4ta	3.0	0.0	−9.6
4tb	4.4	1.5	−9.5
4tc	1.8	1.6	−6.7
4td	3.8	2.8	−7.6
4ca	0.0	0.3	−6.3
4cb	2.8	0.6	−8.8

[a] Obtained by difference between the free energies in Cl_3CH and in vacuo.

corresponds to **4ta**. Only **4tc** and **4ca** have a strong HB O9–H···O5 (bond length=1.85Å), and O9–H···O6 (bond length=1.85 Å), respectively.

As before (model **1**), in vacuo, most stable species are those with strong HB. The energy follows the order **4ca**<**4tc**<**4cb**<**4ta**<**4td**<**4tb**, consistent with the greater strength of intramolecular HB. The biggest difference is that in this case the *cis* (**4ca**) arrangement has a lower energy than the *trans* (**4ta**–**4td**). Again, the inclusion of the solvent (Cl_3CH) produces a strong stabilization of all species (between 6.3 and 9.6 kcal/mol). This stabilization is less than in model **1**, since the presence of three *N*-methyl groups instead of three hydrogen atoms decreases the polarity of the compound. This stabilization is less in species with strong intramolecular HB (see **4ca** and **4tc**), and intramolecular HB are not crucial to establish the most stable conformation. In this situation, the most stable specie corresponds to **4ta**, closely followed by **4ca** (0.3 kcal/mol). This small difference in energy indicates that, in chloroform, the oxalamide **4** will exist as a mixture of the *cis* and *trans* conformers and the ^1H and ^{13}C NMR spectra will be complex and with duplication of signals.

*3.2.3. Model **5**: N,N′-bis(2-hydroxyethyl)-N,N′-dimethyloxalamide.* This is the most complex of all the compounds studied. There are four conformations resulting from rotation of the amide bonds (ω_1 and ω_3 in Scheme 4), **tt**, **cc**, **tc**, and **ct**. In this case, because the substituents on nitrogen atoms are the same, the conformations **tc** and **ct** are equivalent, leaving only three different conformations. However, due to loss of planarity in the oxalamide group, each of these three conformations adopts two staggered arrangements resulting from rotation of the CO–CO bond (see model **3** and model **4**).

For **cc**, **ct**, and **tt** conformers, an exhaustive conformational study in vacuo, DMSO, and CH_3OH was made. For each conformer, there are an enormous amount of rotamers resulting from rotation of the $-CH_2CH_2OH$ chains. In order to simplify we show only one of these rotamers for each conformer and corresponds to the more stable found in DMSO (**5cc**, **5ct**, and **5tt** in Fig. 6 and Table 5).

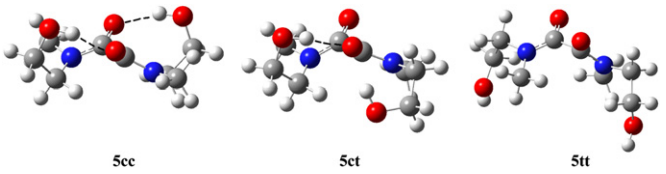

Fig. 6. Geometries of the more relevant stationary points involved in the conformational study of *N*,*N*′-bis(2-hydroxyethyl)-*N*-*N*′-dimethyloxalamide (**5**) in DMSO. Strong HB are shown.

The three conformers **5cc**, **5ct**, and **5tt** all adopt a staggered arrangement of the oxalamide group (dihedral angle O=C–C=O between 100° and 112° in DMSO). There are no large geometric variations with different solvents. However, the inclusion of the solvent produces a strong stabilization of all species and a considerable variation of energies (see Table 5).

Table 5
B3LYP/6-31G** Relative free energies (ΔG, in kcal/mol, 298.15 K, 1 atm) in vacuo (ΔG_{vacuo}), DMSO (ΔG_{DMSO}), CH_3OH (ΔG_{Cl_3CH}) and free energies of solvation (ΔG_{sol}) of the stationary points involved in the conformational study of *N,N′*-bis(2-hydroxyethyl)-*N*-*N′*-dimethyloxalamide (**5**)

	ΔG_{vacuo}	ΔG_{DMSO}	ΔG_{sol}[a]	ΔG_{Cl_3CH}	ΔG_{sol}[b]
5cc	0.0	0.0	−11.1	0.2	−11.1
5ct	1.7	0.3	−12.6	0.4	−12.6
5tt	6.2	0.9	−16.4	0.0	−17.5

[a] Obtained by difference between the free energies in DMSO and in vacuo.
[b] Obtained by difference between the free energies in CH_3OH and in vacuo.

The symmetric conformation **5cc** has two identical strong HB O9–H···O6 and O12–H···O5 (eight-membered rings) with a bond length of 1.85 Å, being the most stable conformer in vacuo and in DMSO. The asymmetric conformation **5ct** has only one strong HB O9–H···O6 (eight-membered rings) with a bond length of 1.86 Å. Finally, the symmetric conformation **5tt**, with no hydrogen bridges, is very unstable in vacuo, but is the most stable conformation in CH_3OH.

3.2.3.1. ^{13}C and ^{1}H NMR study of N,N′-bis(2-hydroxyethyl)-N,N′-dimethyloxalamide. As calculated above (Table 5), in solution **5**[27] can be found as mixture of three conformers (**cc**, **ct**/**tc**, and **tt**). Each of these conformations will have a large number of rotamers resulting from rotation of the $-CH_2CH_2OH$ chain. Due to the high rotational barrier of the amide bond, the three conformers, **cc**, **ct**/**tc**, and **tt**, present different signals and the ^{1}H and ^{13}C NMR spectra will be complex. Because of the symmetry, **cc** and **tt** conformers will have half of the signals. However the **ct**/**tc** conformer presents different signals for each of the amide fragments. In this section we intend to make an assignment of the observed experimental signals in ^{13}C and ^{1}H NMR spectra, for each of the conformers. The experimental spectroscopic data for the compound were recorded in DMSO-d_6 and CD_3OD (see Supplementary data).

The ^{13}C NMR spectra in DMSO-d_6 show sixteen signals. The amidic carbon chemical shifts (C2/C3) appear at 165 ppm as four signals. The signals of C8/C11 atoms are observed at 58 ppm, again as four signals. The C7/C10 signals appear at 52 ppm (two signals) and 48 ppm (two signals). Finally, the carbons of the *N*-methyl groups (C13/C14) are shown as four signals, two at 36 ppm and two more at 32 ppm. This is consistent with a mixture of **cc**, **ct**/**tc**, and **tt** conformers. Four signals for each of the symmetrical conformers (**cc** and **tt**) and eight signals for the asymmetric conformer (**ct**/**tc**).

Molecular orbital calculations can be used to good estimates ^{13}C NMR chemical shifts. Ab initio and DFT calculation of NMR shielding at very accurate levels of approximation are available in literature.[28–31] The GIAO method, implemented in the Gaussian package, is now widely used for these purposes. Good quality shielding results depend on the quality of the basis sets selected. Excellent results are obtained using B3LYP as DFT method and 6-311++G** as basis set.[30] The NMR calculations yield absolute shielding constants (σ) while experimental data is typically given as relative shielding constants (δ) to the tetramethylsilane (TMS).

Eq. 1 is used to convert computed absolute shieldings (σ_{calcd}), to computed relative shieldings (δ_{calcd}), which can be used to compare to the experimentally measured relative shieldings (δ_{exp}).

$$\delta_{calcd} = I + S\sigma_{calcd} \quad (1)$$

The variable *I* represent the shielding of the TMS, and ideally *S* is −1 for ^{13}C shifts. The best results are achieved when *I* and *S* are empirically determined by regressing σ_{calcd} against δ_{exp} over a diverse set of organic compounds. *I* is the resulting intercept of the regression equation and *S* is the slope. We have used for *I* and *S* the values of 175.0 and −0.961, respectively.[30]

Table 6 shows the values of computed relative shieldings (δ_{calcd}), experimentally assigned relative shieldings (δ_{exp}) and differences (Dif.) between the value calculated and experimental for the structures **5cc**, **5ct**, and **5tt** in DMSO.

It should be noted that these calculations are referred to the static molecule as represented in Fig. 6, while experimental NMR spectra are averages affected by dynamic processes, such as conformational equilibrium. Remember that each of these structures, has several rotamers resulting from rotation of the side chain ($-CH_2CH_2OH$) and the CO–CO bond. The discrepancy between calculated and experimental values may be due to the contribution of various rotamers in the experimental value.

As you can see from the Table 6, the calculated and experimental values for **5cc** are practically the same. This may indicate that rotamer **5cc** is probably the largest contribution to the conformer **cc**. However, **5tt** presents a greater difference between the experimental and theoretical values. This indicates the contribution to the **tt** conformer of the structure **5tt** and other rotamers. The major discrepancy (7 ppm) is in the C8/C10 carbons. These carbons are adjacent to the hydroxyl group and are very sensitive to conformational changes of the side chain. Finally, the asymmetric structure **5ct**, has a side (left side in the Fig. 6) identical to both sides of the **5cc** structure, and shows little discrepancy between the experimental and calculated values. Again, the right side (see Fig. 6), similar to both sides of the **5tt** structure, presents a greater difference.

Table 6
^{13}C NMR δ shift (ppm) calculated (δ_{calcd}; B3LYP/6-311++G**), experimental (δ_{exp}) and difference (Dif.) in DMSO for **5cc**, **5ct**, and **5tt**

	δ_{calcd}	δ_{exp}	Dif.
5cc			
C2/C3	166	165	1
C8/C11	58	58	0
C7/C10	52	52	0
C13/C14	31	32	−1
5tt			
C2/C3	166	165	1
C8/C11	65	58	7
C7/C10	48	48	0
C13/C14	38	36	2
5ct			
C2	166	165	1
C8	59	58	1
C7	51	52	−1
C13	30	32	−2
C3	170	165	5
C11	61	58	3
C10	49	48	1
C14	33	36	−3

Despite the discrepancies, it is noteworthy that the carbons adjacent to nitrogen atoms (C7/C10) are not altered by the presence of several rotamers. The chemical shift of these carbons can be accurately calculated and can be used for the assignment of the different conformers resulting from rotation of the amide bond. For example, in this case the C7/C10 signals appear at 52 (±1) ppm when the amide bond adopt a *cis* conformation (see **5cc** and left side of **5ct**) and at 48 (±1) ppm when the amide bond adopt a *trans* arrangement (see **5tt** and right side of **5ct**). Also, although with less precision, chemical shifts of the *N*-methyl groups (C13/C14) can be used.

The ^{1}H NMR spectra, in DMSO-d_6 (500 MHz), show several signals (the assignments are based in the analysis of the COSYGPSW and $^{1}H–^{13}C$ HSQC spectra). The hydroxyl protons appear at 4.74–4.82 ppm as a multiplet. A careful analysis shows that this multiplet is formed by the overlap of four triplets, each with coupling constants of about 5.5 Hz. The triplet is a consequence of the hydroxyl proton coupling with the vicinal CH_2 group. This type of coupling is easily observable, due to slow exchange of hydroxyl

protons in DMSO at room temperature. The complex multiplet signal between 3.50 and 3.57 ppm correspond to the methylene protons C8–H_2 and C11–H_2, coupled with the hydroxyl proton and methylene protons adjacent to nitrogen atom. At 3.38 and 3.25 ppm are two quadruplets, which correspond to the protons adjacent to nitrogen atom (C7–H_2/C10–H_2). Each of these quadruplets is really two overlapping triplets (J 5.5 Hz) centered at 3.39/3.38 ppm and 3.26/3.25 ppm, respectively (see spectrum at 300 MHz in DMSO-d_6 and at 500 MHz in CD_3OD). Finally, the N–CH_3 signals appear at 2.928, 2.920, 2.888, and 2.882 ppm as four singlets.

In the ^{1}H NMR spectra, in CD_3OD (500 MHz), the hydroxyl protons appear at 4.83 ppm as a singlet. The multiplet signal between 3.69 and 3.77 ppm correspond to the methylene protons C8–H_2 and C11–H_2. This signal can be separated in four triplets (J 5.5 Hz). The quadruplet at 3.55 ppm (two triplets overlapped) and the two triplets at 3.45/3.43 ppm correspond to the methylene protons C7–H_2/C10–H_2. The N–CH_3 signals are shown at 3.087, 3.069, 3.030, and 3.019 ppm as four singlets. Again, this is consistent with a mixture of **cc**, **ct**/**tc**, and **tt** conformers.

The ^{1}H–^{13}C HSQC spectra (in DMSO-d_6) shows the correlation between the signals 3.50–3.57(^{1}H)/58(^{13}C), 3.38(^{1}H)/48(^{13}C), 3.25 (^{1}H)/52(^{13}C), 2.928(^{1}H)/35.52(^{13}C), 2.920(^{1}H)/36.05(^{13}C), and 2.888, 2.882(^{1}H)/31.92, 31.72(^{13}C). The ^{13}C signals at 52 (C7/C10) and 32 (N–CH_3) ppm correspond to the *cis* arrangement of the amide bond (see above), and therefore the ^{1}H signals at 3.26/3.25 and 2.888/2.882 ppm can be assigned to protons C7–H_2/C10–H_2, and N–CH_3 in the *cis* amide conformation. Similarly ^{1}H signals at 3.39/3.38 and 2.928/2.920 ppm can be assigned to protons C7–H_2/C10–H_2 and N–CH_3 in the *trans* amide conformation.

The assignment of the methyl groups can be done with a careful analysis of the ^{1}H NMR spectra. The integral relationship between the two central methyl signals is practically the same in DMSO-d_6 (signals at 2.920 and 2.888 ppm) and CD_3OD (signals at 3.069 and 3.030 ppm). These signals can therefore be assigned to **ct**/**tc** conformer. The signal at 2.928 ppm in DMSO-d_6 (3.087 in CD_3OD) correspond to the two N–CH_3 of the **tt** conformer, and also the signal at 2.882 ppm in DMSO-d_6 (3.019 in CD_3OD) can be assigned to the two N–CH_3 of the **cc** conformer (see Table 7).

Table 7
^{1}H NMR δ shift (ppm) and multiplicity (J in Hz) in DMSO-d_6 for **cc**, **tt**, and **ct** conformers of the *N*,*N*′-bis(2-hydroxyethyl)-*N*,*N*′-dimethyloxalamide (**5**)

	cc	**tt**	**ct**
OH	4.74–4.82 (t, J=5.5)	4.74–4.82 (t, J=5.5)	4.74–4.82 (t, J=5.5)
C7–H_2/C10–H_2	3.25 (t, J=5.5)	3.38 (t, J=5.5)	3.25/3.38 (two t, J=5.5)
C8–H_2/C11–H_2	3.50–3.57 (m)	3.50–3.57 (m)	3.50–3.57 (m)
C13–H_3/C14–H_3	2.882 (s)	2.928 (s)	2.888/2.920 (two s)

4. Conclusions

The conformational properties of some *N*-alkyl, *N*,*N*′-dialky and tetraalkyloxalamides have been investigated, in vacuo and in solvent (Cl_3CH, DMSO, CH_3OH), using DFT methods at the B3LYP/63-1G** computational level, have been given a special emphasis on oxalamides with substituents of the type $-CH_2CH_2OH$.

The rotation of each CO–N amide bond originates two different conformers, *cis* and *trans*. On the other hand, CO–CO torsion angle angle may vary from 0° (*s-cis*) to 180° (*s-trans*) producing different rotamers. Finally, the rotation of side chain ($-CH_2CH_2OH$), gives rise to numerous additional rotamers.

In vacuo or in solvent, the geometrical results are similar; however inclusion of solvent produces a strong stabilization of all species and a considerable variation of energies.

In oxalamides with the N–H group (*N*-alkyl and *N*,*N*′-dialky), the most stable conformations are those in which the oxalamide moiety adopts a planar *s-trans* (CO–CO bond=180°) arrangement and the all amide bonds are *trans*. In these cases there is only one preferred conformation and NMR spectra show no duplication of signals.

With substituents of the type $-CH_2CH_2OH$, most stable rotamers (in vacuo) are those with strong intramolecular HB. However in solvent, HB are not crucial to establish the most stable specie and depend on the solvent used.

A different situation shows tetraalkyloxalamides, in which the oxalamide moiety always adopts a skewed arrangement (O=C–C=O dihedral $\neq$180°). The theoretical study done on the tetramethyloxalamide shows that the rotational barrier around the CO–N amide bond is high (ΔG_{Cl_3CH}=22.23 kcal/mol). These numerical results can be extrapolated to the other oxalamides. Because of hindered rotation about this CO–N amide bond, each of the resultant different conformers (*cis* and *trans*) can be observed in the NMR spectra. As a result of the loss of planarity of oxalamide system, each conformer, have several rotamers from the rotation of the CO–CO bond. However, the low free energy barrier (ΔG_{Cl_3CH}=7.08 kcal/mol) associated to this rotation allow for a rapid exchange between these rotamers at room temperature and do not cause different signals in the NMR spectrum. There is also a fast exchange between rotamers resulting from rotation of the side chain ($-CH_2CH_2OH$). Again, the most stable rotamers in vacuo (but not in solvent) are those with strong intramolecular HB. The *cis* or *trans* disposition of the CO–N amide bond have similar energies and the result is a mixture of conformers that can be individually observed in NMR spectra. A careful study of ^{13}C and ^{1}H NMR spectra together with theoretical calculations (GIAO method) allow the assignment of the signals of each of these conformers.

Acknowledgements

This work was supported by research funds provided by the Ministerio de Ciencia e Innovación of the Spanish Government (project CTQ2009-11027/BQU).

Supplementary data

Tables S1–S5. Cartesian coordinates for transition states: **TS1**, **TS2***syn*, and **TS2***anti*. Synthesis and some data of model **5**: *N*,*N*′-bis(2-hydroxyethyl)-*N*,*N*′-dimethyloxalamide. ^{1}H NMR and ^{13}C NMR spectra of *N*,*N*′-bis(2-hydroxyethyl)oxalamide in DMSO-d_6. ^{1}H NMR, ^{13}C NMR, ^{1}H–^{1}H COSYGPSW, and ^{1}H–^{13}C HSQC spectra of *N*,*N*′-bis(2-hydroxyethyl)-*N*,*N*′-dimethyloxalamide in DMSO-d_6 and in CD_3OD. Supplementary data related to this article can be found online at doi:10.1016/j.tet.2011.03.075. These data include MOL files and InChIKeys of the most important compounds described in this article.

References and notes

1. (a) Alemán, C. *Proteins* **1997**, *29*, 575; (b) Alemán, C.; Puiggalí, J. *J. Org. Chem.* **1995**, *60*, 910; (c) Alemán, C.; Puiggalí, J. *J. Polym. Sci., Part B: Polym. Phys.* **1996**, *34*, 1327.
2. (a) Chorev, M.; Yacon, M.; Wormser, U.; Levian-Teitelbaun, D.; Gilon, C.; Selinger, Z. *Eur. J. Med. Chem.* **1986**, *21*, 96; (b) Pallai, P.; Struthers, S.; Goodman, M.; Moroderi, M.; Wunch, E.; Vale, W. *Biochemistry* **1985**, *24*, 1933; (c) Rodriguez, M.; Dubreil, P.; Bali, J.-P.; Martinez, J. *J. Med. Chem.* **1987**, *30*, 758; (d) Goodman, M.; Coddington, J.; Mierke, D. F.; Fuller, W. D. *J. Am. Chem. Soc.* **1987**, *109*, 4712.
3. (a) Puiggalí, J.; Aceituno, J. E.; Navarro, J. L.; Campos, L.; Subirana, J. A. *Macromolecules* **1996**, *29*, 8170; (b) Navarro, E.; Puiggalí, J.; Subirana, J. A. *Macromol. Chem. Phys.* **1995**, *96*, 2361; (c) Alemán, C.; Franco, L.; Puiggalí, J. *Macromolecules* **1994**, *27*, 4298.
4. (a) Shalaby, S. W.; Pearce, E. M.; Fredericks, R. J.; Turi, E. A. *J. Polym. Sci., Polym. Phys. Ed.* **1973**, *11*, 1; (b) Chatani, Y.; Ueda, Y.; Tadokoro, H.; Deits, W.; Vogl, O. *Macromolecules* **1978**, *11*, 636; (c) Gaymans, R. J.; Venkatraman, V. S.; Schüijer, S. *J. Polym. Sci., Polym. Chem. Ed.* **1984**, *22*, 1373; (d) Franco, L.; Subirana, J. A.; Puiggalí, J. *Macromolecules* **1998**, *31*, 3912.
5. Frkanec, L.; Zinic, M. *Chem. Commun.* **2010**, 522.

6. Padilla-Martinez, I. I.; Martinez-Martinez, F. J.; Guillén-Hernandez, C. I.; Chaparro-Huerta, M.; Cabrera-Pérez, L. C.; Gomez-Castro, C. Z.; López-Romero, B. A.; García-Báez, E. V. *Arkivoc* **2005**, *vi*, 401.
7. Martínez-Martínez, F. J.; Ariza-Castolo, A.; Tlahuext, H.; Tlahuextl, M.; Contreras, R. *J. Chem. Soc., Perkin Trans. 2* **1993**, 1481.
8. Martínez-Martínez, F. J.; Padilla-Martinez, I. I.; Brito, M. A.; Geniz, E. D.; Rojas, R. C.; Saavedra, J. B. R.; Höpfl, H.; Tlahuextl, M.; Contreras, R. *J. Chem. Soc., Perkin Trans. 2* **1998**, 401.
9. Verardo, G.; Giumanini, A. G.; Gorassini, F.; Tolazzi, M.; Strazzolini, P. *Tetrahedron* **1993**, *49*, 10609.
10. Cerioni, G.; Glumanini, A. G.; Verardo, G. *J. Phys. Org. Chem.* **1998**, *11*, 387.
11. Katritzky, A.; Levell, J.; Pleynet, D. *Synthesis* **1998**, 153.
12. Aleman, C.; Puiggali, J. *J. Org. Chem.* **1999**, *64*, 351.
13. Armelin, E.; Aleman, C.; Puiggali, J. *J. Org. Chem.* **2001**, *66*, 8076.
14. Frisch, M. J.; Trucks, G. W.; Schlegel, H. B.; Scuseria, G. E.; Robb, M. A.; Cheeseman, J. R.; Montgomery, J. A., Jr.; Vreven, T.; Kudin, K. N.; Burant, J. C.; Millam, J. M.; Iyengar, S. S.; Tomasi, J.; Barone, V.; Mennucci, B.; Cossi, M.; Scalmani, G.; Rega, N.; Petersson, G. A.; Nakatsuji, H.; Hada, M.; Ehara, M.; Toyota, K.; Fukuda, R.; Hasegawa, J.; Ishida, M.; Nakajima, T.; Honda, Y.; Kitao, O.; Nakai, H.; Klene, M.; Li, X.; Knox, J. E.; Hratchian, H. P.; Cross, J. B.; Adamo, C.; Jaramillo, J.; Gomperts, R.; Stratmann, R. E.; Yazyev, O.; Austin, A. J.; Cammi, R.; Pomelli, C.; Ochterski, J. W.; Ayala, P. Y.; Morokuma, K.; Voth, G. A.; Salvador, P.; Dannenberg, J. J.; Zakrzewski, V. G.; Dapprich, S.; Daniels, A. D.; Strain, M. C.; Farkas, O.; Malick, D. K.; Rabuck, A. D.; Raghavachari, K.; Foresman, J. B.; Ortiz, J. V.; Cui, Q.; Baboul, A. G.; Clifford, S.; Cioslowski, J.; Stefanov, B. B.; Liu, G.; Liashenko, A.; Piskorz, P.; Komaromi, I.; Martin, R. L.; Fox, D. J.; Keith, T.; Al-Laham, M. A.; Peng, C. Y.; Nanayakkara, A.; Challacombe, M.; Gill, P. M. W.; Johnson, B.; Chen, W.; Wong, M. W.; Gonzalez, C.; Pople, J. A. *Gaussian 03, Revision C. 02*; Gaussian: Wallingford CT, 2004.
15. (a) Parr, R. G.; Yang, W. *Density Functional Theory of Atoms and Molecules*; Oxford University: New York NY, 1989; (b) Ziegler, T. *Chem. Rev.* **1991**, *91*, 651.
16. (a) Becke, A. D. *J. Chem. Phys.* **1993**, *98*, 5648; (b) Lee, C.; Yang, W.; Parr, R. G. *Phys. Rev. B* **1988**, *37*, 785.
17. Hehre, W. J.; Radom, L.; Schleyer, P. v. R.; Pople, J. A. *Ab Initio Molecular Orbital Theory*; Wiley: New York, NY, 1986.
18. (a) Tomasi, J.; Persico, M. *Chem. Rev.* **1994**, *94*, 2027; (b) Simkin, B. Y.; Sheikhet, I. *Quantum Chemical and Statistical Theory of Solutions-A Computational Approach*; Ellis Horwood: London, 1995.
19. (a) Cances, E.; Mennunci, B.; Tomasi, J. *J. Chem. Phys.* **1997**, *107*, 3032; (b) Cossi, M.; Barone, V.; Cammi, R.; Tomasi, J. *Chem. Phys. Lett.* **1996**, *255*, 32; (c) Barone, V.; Cossi, M.; Tomasi, J. *J. Comput. Chem.* **1998**, *19*, 404.
20. Temeriusz, A.; Rowinska, M.; Piekarska-Bartoszewicz, B. *Carbohydr. Res.* **2005**, *340*, 1656.
21. Gomez-Castro, C. Z.; Padilla-Martinez, I. I.; Martinez-Martinez, F. J.; García-Báez, E. V. *Arkivoc* **2008**, *v*, 227.
22. Hope, D. B.; Horncastle, K. C. *Biochem. J.* **1967**, *102*, 910.
23. Neveux, M.; Bruneau, C.; Lecolier, S.; Dixneuf, P. *Tetrahedron* **1993**, *49*, 2629.
24. Bennet, A. J.; Somayaji, V.; Brown, R. S.; Santarsiero, B. D. *J. Am. Chem. Soc.* **1991**, *113*, 7563.
25. Desseyn, H. O.; Perlepes, S. P.; Clou, K.; Blaton, N.; Van der Veken, B. J.; Dommisse, R.; Hansen, P. E. *J. Phys. Chem. A* **2004**, *108*, 5175.
26. Mujika, J. I.; Matxain, J. M.; Eriksson, L. A.; Lopez, X. *Chem.—Eur. J.* **2006**, *12*, 7215.
27. Synthesized according to the procedure described by us: Testa, M. L.; Antista, L.; Mingoia, F.; Zaballos-García, E. *J. Chem. Res.* **2006**, *3*, 182.
28. Barfield, M.; Fagerness, P. *J. Am. Chem. Soc.* **1997**, *119*, 8699.
29. Jaroszewska-Manaj, J.; Maciejewska, D.; Wawer, I. *Magn. Reson. Chem.* **2000**, *38*, 482.
30. Giesen, D. J.; Zumbulyadis, N. *Phys. Chem. Chem. Phys.* **2002**, *4*, 5498.
31. Azizi, S. N.; Esmaili, C. *World Appl. Sci. J.* **2009**, *7*, 559.